

# Optimization of Mixed Conducting Properties of $Y_2O_3-ZrO_2-TiO_2$ and $Sc_2O_3-Y_2O_3-ZrO_2-TiO_2$ Solid Solutions as Potential SOFC Anode Materials

Shanwen Tao and John T. S. Irvine<sup>1</sup>

*School of Chemistry, University of St. Andrews, Fife KY16 9ST, Scotland, United Kingdom*

Received August 17, 2001; in revised form November 7, 2001; accepted December 3, 2001

The mixed conductor  $Y_{0.2}Zr_{0.62}Ti_{0.18}O_{1.9}$  is a promising candidate as an SOFC anode material. In order to further improve the ionic conductivity, the conductivity of system  $Sc_2O_3-Y_2O_3-ZrO_2-TiO_2$  was investigated when Y was substituted by Sc. Materials with single cubic fluorite structure were prepared by solid state reaction. The ionic and electronic conductivities were measured by four-terminal dc method in 5%  $H_2$  and ac impedance spectroscopy in air and 5%  $H_2$  respectively. It was found that  $TiO_2$  may dissolve to about 18 mol% in the ternary systems  $Y_2O_3-ZrO_2-TiO_2$  and  $Sc_2O_3-ZrO_2-TiO_2$ , and 20 mol% in the quaternary system  $Sc_2O_3-Y_2O_3-ZrO_2-TiO_2$ . It was also observed that the ionic conductivity is related to the oxygen vacancy concentration and the size of doped ions, and electronic conductivity to the lattice parameter, the sublattice ordering, and the degree of Ti substitution. In addition, both the ionic and electronic conductivities have been improved by the introduction of scandium into the  $Y_2O_3-ZrO_2-TiO_2$  system. The highest ionic conductivity ( $1.0 \times 10^{-2}$  S/cm at 900°C) and electronic conductivity (0.14S/cm at 900°C) were observed for  $Sc_{0.2}Zr_{0.62}Ti_{0.18}O_{1.9}$  and  $Sc_{0.1}Y_{0.1}Zr_{0.6}Ti_{0.2}O_{1.9}$ , respectively. Considering the required levels of both ionic and electronic conductivities for ideal SOFC anode materials,  $Sc_{0.15}Y_{0.05}Zr_{0.62}Ti_{0.18}O_{1.9}$  is a promising candidate with ionic and electronic conductivities  $7.8 \times 10^{-3}$  and  $1.4 \times 10^{-1}$  S/cm, respectively, at 900°C. © 2002 Elsevier Science (USA)

## 1. INTRODUCTION

Fuel cells offer a means of electrochemical conversion of hydrogen or hydrocarbon fuels (such as methane) to produce electricity. The solid oxide fuel cell (SOFC) is one of the most promising candidate fuel cell systems and is an all-ceramic device operating at high temperatures. Present development of SOFCs is based mainly on the

yttria-stabilized zirconia (YSZ) electrolyte because it exhibits good thermal and chemical stability, high oxide ion conductivity, and mechanical strength at high temperature (1). The most commonly used anode materials for zirconia-based SOFCs are Ni/ZrO<sub>2</sub> cermets, which display excellent catalytic properties for fuel oxidation and good current collection but do exhibit disadvantages, such as low tolerance to sulfur (2) and carbon deposition (3) when using hydrocarbon fuels and poor oxidative cycling. The introduction of early transition metal oxides, e.g., TiO<sub>2</sub>, into a zirconia solid solution for use as anode materials is a very promising strategy. Such materials display reasonable electrochemical activity that is comparable to that of ceria doped with 40% Gd (4). For an ideal anode material, the property of mixed conduction under fuel conditions is very important because this allows the electrochemical reactions to occur over the entire electrode–fuel interface as opposed to solely at the electrolyte, electrode, and fuel gas three-phase boundary (TPB) in the current cermet materials (5, 6). There have been some previous reports about phase relations and conductivity of the  $Y_2O_3-ZrO_2-TiO_2$  system (7–9); however, these have essentially focused upon TiO<sub>2</sub> doping of 8 and 10 mol% Y<sub>2</sub>O<sub>3</sub>-doped zirconia. Our previous investigation focused on the entire  $Y_2O_3-ZrO_2-TiO_2$  system and revealed that the cubic fluorite structure of YSZ can be maintained even at higher titanium contents up to 18 atom%, while still maintaining fairly low Y<sub>2</sub>O<sub>3</sub> concentrations (10, 11). In this study, the conductivity of  $Y_xZr_{0.82-x}Ti_{0.18}O_{2-x/2}$  with  $x = 0.16, 0.18,$  and  $0.2$  has been investigated. In order to further optimize the ionic conductivity, scandium was introduced to the system because the size of Sc<sup>3+</sup> dopant is much closer to Zr<sup>4+</sup> than Y<sup>3+</sup> ions. This results in Sc-stabilized ZrO<sub>2</sub> (ScSZ) exhibiting much higher ionic conductivity than YSZ (12–14). Therefore, in this work, the ionic and electronic conductivities of the  $Sc_2O_3-Y_2O_3-ZrO_2-TiO_2$  system have

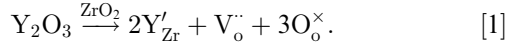
<sup>1</sup>To whom correspondence should be addressed. Fax: +44 1334 463808. E-mail: [jtsi@st-andrews.ac.uk](mailto:jtsi@st-andrews.ac.uk).

been studied as well. The possible factors that may affect the mixed conduction are also discussed.

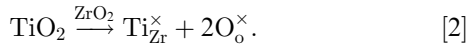
## 2. DETERMINATION OF IONIC AND ELECTRONIC CONDUCTIVITIES

Previous measurements show that there is no variation in the total electrical (ionic plus  $n$ -type) conductivity of  $Y_{0.2}Zr_{0.62}Ti_{0.18}O_{1.9}$  above  $10^{-14}$  atm at  $930^\circ\text{C}$  (10), indicating that the electrical conductivity of the samples in air is dominated by oxide ion conductivity. In high  $pO_2$ , e.g., in air,  $Ti^{4+}$  is not reduced and so, it is supposed that the electronic conductivity is negligible. Under reducing conditions, electronic conduction is dominant when Ti content is significant. The relationship between electronic conductivity and  $pO_2$  may be derived from Brouwer's approach (15) using Kroger-Vink notation.

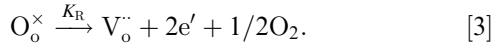
Oxygen vacancies may be introduced when dissolving  $Y_2O_3$  into the  $ZrO_2$  lattice:



When further introducing  $TiO_2$  into the  $Y_2O_3$ - $ZrO_2$  system, it is expected that some  $Zr^{4+}$  ions may be substituted by  $Ti^{4+}$  ions as they possess the same electronic charge



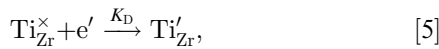
Under a reducing atmosphere, some lattice oxygen may be released as follows:



The corresponding mass action equation is

$$K_R(T) = [V_o^{\cdot\cdot}]n^2pO_2^{1/2}, \quad [4]$$

where  $n$  is the concentration of electronic carriers. The creation of these electronic defects is closely related with the reduction of Ti, thus,



which gives the mass action relation

$$K_D(T) = \frac{[Ti'^{\cdot}_{Zr}]}{[Ti^{\times}_{Zr}]n}. \quad [6]$$

The electroneutrality condition for the  $Y_2O_3$ - $ZrO_2$ - $TiO_2$  system is

$$[Y'_{Zr}] + [Ti'^{\cdot}_{Zr}] = 2[V_o^{\cdot\cdot}]. \quad [7]$$

The mass balance for titanium species is

$$[Ti]_{\text{total}} = [Ti'^{\cdot}_{Zr}] + [Ti^{\times}_{Zr}]. \quad [8]$$

Because only small amounts of  $Ti^{4+}$  ions were reduced at reducing atmospheres, it is assumed that  $[Ti'^{\cdot}_{Zr}] \ll [Ti^{\times}_{Zr}]$ ;  $[Ti'^{\cdot}_{Zr}] \ll [Y'_{Zr}]$ . Equations [7] and [8] may be simplified as

$$[Y'_{Zr}] \cong 2[V_o^{\cdot\cdot}] \quad [9]$$

$$[Ti]_{\text{total}} \cong [Ti^{\times}_{Zr}]. \quad [10]$$

Combining Eqs. [4], [6], [9] and [10], it is deduced that,

$$[Ti'^{\cdot}_{Zr}] = K_D(2K_R)^{1/2}[Ti]_{\text{total}}[Y'_{Zr}]^{-1/2}pO_2^{-1/4}. \quad [11]$$

In the equation above,  $K_D$ ,  $K_R$ ,  $[Ti]_{\text{total}}$ , and  $[Y'_{Zr}]$  are constant, therefore,

$$[Ti'^{\cdot}_{Zr}] \propto pO_2^{-1/4}. \quad [12]$$

In a reducing atmosphere, the electronic conduction in the  $Sc_2O_3$ - $Y_2O_3$ - $ZrO_2$ - $TiO_2$  system is due to a polaronic mechanism. Electrons may hop from  $[Y'_{Zr}]$  to the adjacent titanium cations. The relationship between electronic conductivity and the concentration of charge-carrier electrons is

$$\sigma_e = n_e q_e \mu_e, \quad [13]$$

where  $n_e$  is the number of mobile electrons per unit volume ( $\text{cm}^3$ ),  $q_e$  is  $e$  for elementary charge of electron carriers, and  $\mu_e$  is the mobility of electrons. Assuming  $\mu_e$  is constant in a  $Sc$ - $Y$ - $Zr$ - $Ti$ - $O$  solid solution with constant chemical composition,  $pO_2$ , and temperature, then the electronic conductivity is proportional to  $n_e$ , i.e.,  $\sigma_e \propto n_e$ . Obviously, in a reducing atmosphere,  $n_e \propto [Ti'^{\cdot}_{Zr}]$ . Thus,

$$\sigma_e \propto n_e \propto [Ti'^{\cdot}_{Zr}] \propto pO_2^{-1/4}. \quad [14]$$

This defect analysis is quite consistent with the results of the four-terminal dc measurement as shown in section 4 (Fig. 11). The electronic contribution  $\sigma_e$  has been given as

$$\sigma_e = \sigma_T - \sigma_i, \quad [15]$$

where  $\sigma_i$  is the conductivity in the  $pO_2$  range when ionic conduction dominates. The slope of  $\sigma_e$  vs  $pO_2$  is quite close to  $-\frac{1}{4}$  in accordance with the assumption that only small amounts of titanium are reduced at low  $pO_2$ , e.g.,  $[Ti'^{\cdot}_{Zr}] \ll [Ti^{\times}_{Zr}]$ . It can be argued that, at low  $pO_2$ , the ionic conductivity of  $Sc$ - $Y$ - $Zr$ - $Ti$ - $O$  samples is not significantly different from that at high  $pO_2$  because the oxygen vacancy concentration change is insignificant compared to the total. Based on the above analysis, it is supposed that, in the ac conductivity measurements, the electrical conductivity in air is  $\sigma_e$  ( $\sigma_e \ll \sigma_i$ ), and in 5%  $H_2$   $\sigma_T$ . The electronic conductivity can therefore be calculated from Eq. [15].

### 3. EXPERIMENTAL

#### 3.1. Sample Preparation

High-purity yttria, scandia, zirconia, and titania were used as the starting materials. Samples were weighed, mixed with acetone and ball-milled in zirconia containers with zirconia balls. After drying and removal of acetone, the mixtures were pressed into pellets (13 mm diameter  $\times$  2 mm thick) at a pressure of 2000 kg cm<sup>-2</sup>. The pellets were calcined at 1000°C for 1 hour, sintered at 1500°C for at least 48 hours as detailed in Table 1, and then air quenched to room temperature from 1200°C. The relative densities for the sintered samples are in the range of 82–92%. The sample used for dc measurement was prepared by crushing the 1500°C pellets, pressing again into a pellet, and sintering at 1300°C for 4 hours. The relative density of the as-prepared pellets is 66%.

#### 3.2. Characterization

Phase purity and unit cell lattice parameters were determined by a Stoe Stadi-P X-ray diffractometer (10–85° 2 $\theta$ , step size 0.02° 2 $\theta$ , CuK $\alpha$  radiation) using silicon as an external calibration standard. For ac impedance measurements, a Schlumberger Solartron 1260 frequency response analyzer coupled with a 1287 electrochemical interface controlled by Z-plot electrochemical impedance software was used over the frequency range 1 MHz to 100 mHz. Measurements were performed in 50°C steps in air and 5% H<sub>2</sub> in Ar, between 600 and 900°C on as-sintered pellets coated with porous Pt electrodes at both sides. The  $p_{\text{H}_2\text{O}}$  of the gases used is about  $8.4 \times 10^{-4}$  atm. The samples were reduced overnight in 5% H<sub>2</sub> at 900°C ( $p_{\text{O}_2} \sim 10^{-22}$  atm) before measuring the total conductivities in 5% H<sub>2</sub> in Ar.

The dc conductivity was measured by a conventional four-terminal method using a Keithley 220 programmable current source to control current and a Schlumberger Solartron 7150 digital multimeter to measure voltage.

### 4. RESULTS AND DISCUSSION

#### 4.1. Y<sub>2</sub>O<sub>3</sub>–ZrO<sub>2</sub>–TiO<sub>2</sub> System

In previous studies, we have examined the extent of cubic fluoride solid solution formation in the system Y<sub>2</sub>O<sub>3</sub>–ZrO<sub>2</sub>–TiO<sub>2</sub> (11), and investigated ionic and electronic conductivity in the system (10). In the initial phase of this study we have re-examined this system, looking more closely at the conducting properties of compositions at the low yttria, high titania limit. Three pure cubic phases, Y<sub>0.16</sub>Zr<sub>0.66</sub>Ti<sub>0.18</sub>O<sub>1.92</sub>, Y<sub>0.18</sub>Zr<sub>0.64</sub>Ti<sub>0.18</sub>O<sub>1.91</sub>, and Y<sub>0.2</sub>Zr<sub>0.62</sub>Ti<sub>0.18</sub>O<sub>1.9</sub>, were prepared by heating the mixed oxides Y<sub>2</sub>O<sub>3</sub>, ZrO<sub>2</sub>, and TiO<sub>2</sub> at 1500°C for 2 days (Table 1).

The conductivities of the samples were measured by ac impedance. It was reported that the low-temperature electrical conductivity of 10 mol% TiO<sub>2</sub>-doped YSZ is significantly affected by the grain boundary, which is related to the firing temperature and time (16) and at higher temperatures the expected relative contribution of the grain boundary will become even smaller. Using a higher sintering temperature was found to reduce this problem (16) and, as our samples have been sintered at 1500°C for a long time, the grain boundary contribution to the total conductivity is insignificant at higher temperatures. Figure 1 shows a typical impedance response of the samples in air. At 400°C, it consists of a slightly distorted semicircle at high frequency and a straight line with a slope of about 45° at low frequency, probably due to the Warburg impedance concerning a semi-infinite diffusion of the charge carriers (17). The geometric capacitance of the semicircle, is  $\sim 6 \times 10^{-12}$  F cm<sup>-1</sup>, is due to the bulk response (18). Therefore, the overall impedance response is dominated by the bulk response at a temperature as low as 400°C. No low-frequency arc was observed in the ac impedance response when measured in 5% H<sub>2</sub>, indicating diffusion or charge transfer limitation, demonstrating that electronic conduction is more important than ionic. Therefore, all the conductivities shown in the following plots are total which is dominated by the bulk contribution.

As shown in Fig. 2, the composition with 16 metal atom% Y exhibits the highest ionic conductivity in air, as would be expected. It is well known that the ionic conductivity of yttria-stabilized zirconia decreases with increasing yttria concentration due to defect association, or more accurately due to defect aggregation and clustering (19). For compositions containing 20 metal atom% Y, or compositions containing close to this level of Y with

**TABLE 1**  
Phase Compositions of Y–Zr–Ti–O and Sc–Y–Zr–Ti–O  
Samples after Heating at 1500°C

Nominal composition	Firing time at 1500°C (hour)	Phase composition
Y <sub>0.2</sub> Zr <sub>0.62</sub> Ti <sub>0.18</sub> O <sub>1.9</sub>	48	Cubic
Y <sub>0.18</sub> Zr <sub>0.64</sub> Ti <sub>0.18</sub> O <sub>1.91</sub>	48	Cubic
Y <sub>0.16</sub> Zr <sub>0.66</sub> Ti <sub>0.18</sub> O <sub>1.92</sub>	48	Cubic
Sc <sub>0.16</sub> Zr <sub>0.66</sub> Ti <sub>0.18</sub> O <sub>1.92</sub>	51	Cubic + ZrTiO <sub>4</sub>
Sc <sub>0.08</sub> Y <sub>0.08</sub> Zr <sub>0.66</sub> Ti <sub>0.18</sub> O <sub>1.92</sub>	51	Cubic + tetragonal
Sc <sub>0.2</sub> Zr <sub>0.62</sub> Ti <sub>0.18</sub> O <sub>1.9</sub>	67	Cubic
Sc <sub>0.15</sub> Y <sub>0.05</sub> Zr <sub>0.62</sub> Ti <sub>0.18</sub> O <sub>1.9</sub>	85	Cubic
Sc <sub>0.1</sub> Y <sub>0.1</sub> Zr <sub>0.62</sub> Ti <sub>0.18</sub> O <sub>1.9</sub>	67	Cubic
Sc <sub>0.05</sub> Y <sub>0.15</sub> Zr <sub>0.62</sub> Ti <sub>0.18</sub> O <sub>1.9</sub>	85	Cubic
Sc <sub>0.2</sub> Zr <sub>0.6</sub> Ti <sub>0.2</sub> O <sub>1.9</sub>	94	Cubic + tetragonal
Sc <sub>0.15</sub> Y <sub>0.05</sub> Zr <sub>0.6</sub> Ti <sub>0.2</sub> O <sub>1.9</sub>	72	Cubic + tetragonal
Sc <sub>0.1</sub> Y <sub>0.1</sub> Zr <sub>0.6</sub> Ti <sub>0.2</sub> O <sub>1.9</sub>	94	Cubic
Sc <sub>0.05</sub> Y <sub>0.15</sub> Zr <sub>0.6</sub> Ti <sub>0.2</sub> O <sub>1.9</sub>	72	Cubic
Sc <sub>0.1</sub> Y <sub>0.1</sub> Zr <sub>0.58</sub> Ti <sub>0.22</sub> O <sub>1.9</sub>	87	Cubic + TiO <sub>2</sub> ?

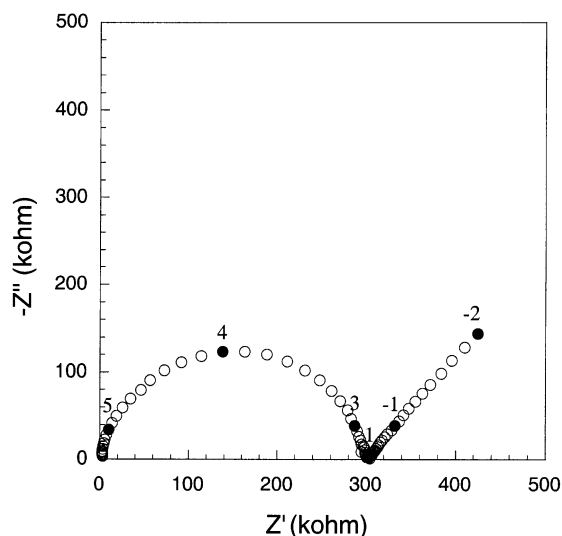


**FIG. 1.** Ac impedance plots,  $-Z''$  versus  $Z'$ , obtained at  $400^\circ\text{C}$  for the  $\text{Sc}_{0.1}\text{Y}_{0.1}\text{Zr}_{0.6}\text{Ti}_{0.2}\text{O}_{1.9}$  sample.

extensive codoping by an additional ion, ionic conductivity would be expected to be in the concentrated region, showing a characteristic high activation energy with no transition to a lower activation energy due to disaggregation of clusters. The ionic conduction activation energy increases with increasing yttria content. Thus, the sample  $\text{Y}_{0.2}\text{Zr}_{0.62}\text{Ti}_{0.18}\text{O}_{1.9}$  exhibits the highest activation energy and lowest ionic conductivity. The presence of titania on the zirconia site slightly decreases the activation energy due to a decrease in the unit cell parameter.

The electronic conductivity of the three samples measured by impedance spectroscopy and corrected using

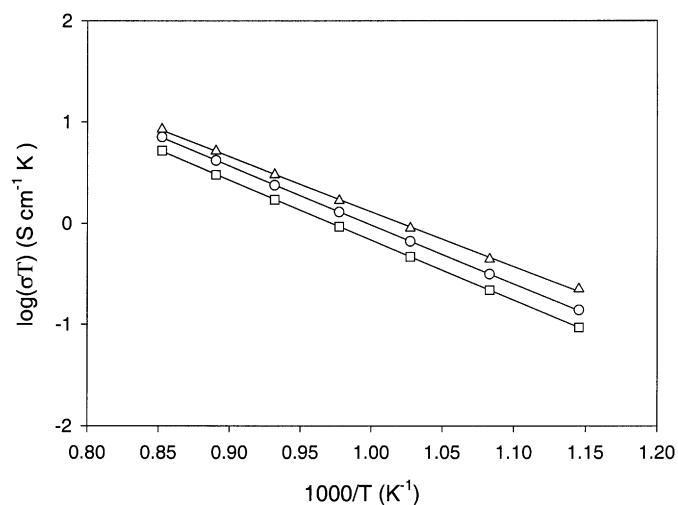


**FIG. 2.** Ionic conductivity of Y-Zr-Ti-O, cubic solid solutions at different temperatures.  $\circ$ ,  $\text{Y}_{0.2}\text{Zr}_{0.62}\text{Ti}_{0.18}\text{O}_{1.9}$ ;  $\square$ ,  $\text{Y}_{0.18}\text{Zr}_{0.64}\text{Ti}_{0.18}\text{O}_{1.91}$ ;  $\triangle$ ,  $\text{Y}_{0.16}\text{Zr}_{0.66}\text{Ti}_{0.18}\text{O}_{1.92}$ .

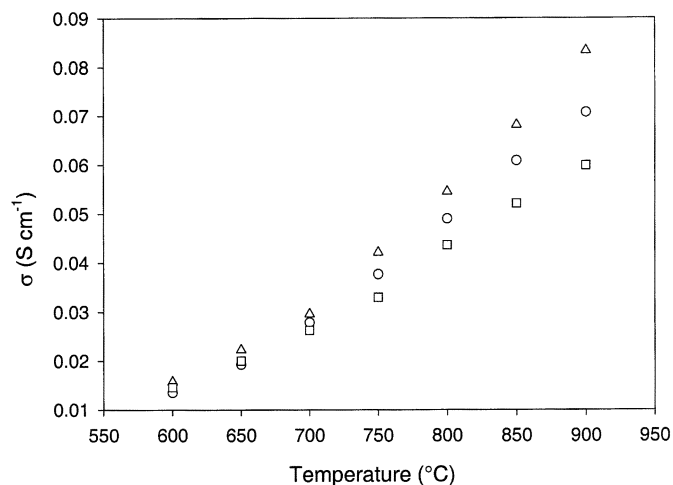


**FIG. 3.** Electronic conductivity of Y-Zr-Ti-O cubic solid solutions at different temperatures.  $\circ$ ,  $\text{Y}_{0.2}\text{Zr}_{0.62}\text{Ti}_{0.18}\text{O}_{1.9}$ ;  $\square$ ,  $\text{Y}_{0.18}\text{Zr}_{0.64}\text{Ti}_{0.18}\text{O}_{1.91}$ ;  $\triangle$ ,  $\text{Y}_{0.16}\text{Zr}_{0.66}\text{Ti}_{0.18}\text{O}_{1.92}$ .

Eq. [15] is shown in Fig. 3. The final conductivity is also corrected by the relative density according to Eq. [16]

$$\sigma = \sigma_{\text{meas}} \frac{\rho_{\text{theor}}}{\rho_{\text{obs}}}, \quad [16]$$

where  $\sigma$  is the real conductivity,  $\sigma_{\text{meas}}$  is measured conductivity, and  $\rho_{\text{theor}}$  and  $\rho_{\text{obs}}$  are theoretical and observed densities. In general, the electronic conductivity is in the range  $10^{-2}$ – $10^{-1}$  S/cm between  $600$  and  $900^\circ\text{C}$ . Samples  $\text{Y}_{0.16}\text{Zr}_{0.66}\text{Ti}_{0.18}\text{O}_{1.92}$  exhibits the highest and  $\text{Y}_{0.2}\text{Zr}_{0.62}\text{Ti}_{0.18}\text{O}_{1.9}$  the lowest electronic conductivity among the three specimens. From the points of both ionic and electronic conductivities, in the tested three compositions,  $\text{Y}_{0.16}\text{Zr}_{0.66}\text{Ti}_{0.18}\text{O}_{1.92}$  is the best as potential SOFC anode material, assuming the difference in their catalytic activity to electrochemical reactions at anode is negligible.

$\text{Sc}_2\text{O}_3$ -stabilized  $\text{ZrO}_2$  (ScSZ) exhibits higher oxide ion conductivity than YSZ because the size of  $\text{Sc}^{3+}$  is closer to  $\text{Zr}^{4+}$  ions than  $\text{Y}^{3+}$  ions (12–14). It is expected that the ionic conductivity could be improved by the introduction of scandium into the Y-Zr-Ti-O system. In addition, the decreased lattice parameters may also benefit the electron hopping and increase electronic conductivity. Therefore, the conductivity of the quaternary Sc-Y-Zr-Ti-O system was investigated.

#### 4.2. $\text{Sc}_2\text{O}_3$ - $\text{Y}_2\text{O}_3$ - $\text{ZrO}_2$ - $\text{TiO}_2$ System

As stated above, the optimum composition in the ternary  $\text{Y}_2\text{O}_3$ - $\text{ZrO}_2$ - $\text{TiO}_2$  system is  $\text{Y}_{0.16}\text{Zr}_{0.66}\text{Ti}_{0.18}\text{O}_{1.92}$  in terms of ionic and electronic conductivities. When Y was replaced by Sc at the 50 and 100% levels, a pure cubic phase was not obtained. After sintering at  $1500^\circ\text{C}$ ,

impurities of tetragonal  $\text{ZrO}_2$ -based solid solution and  $\text{ZrTiO}_4$  were found in the targeted compositions  $\text{Sc}_{0.08}\text{Y}_{0.08}\text{Zr}_{0.66}\text{Ti}_{0.18}\text{O}_{1.92}$  and  $\text{Sc}_{0.16}\text{Zr}_{0.66}\text{Ti}_{0.18}\text{O}_{1.92}$ , respectively (Table 1). From the ternary  $\text{Y}_2\text{O}_3$ - $\text{ZrO}_2$ - $\text{TiO}_2$  phase diagram (11), a pure cubic solid solution phase cannot be approached when the content of  $\text{YO}_{1.5}$  is less than 15 mol%. In the Sc-Zr-Ti-O and Sc-Y-Zr-Ti-O systems, in order to obtain cubic solid solutions, the Sc content has to be higher than 15 mol%. Therefore, the total content of Sc/Y in the Sc-Y-Zr-Ti-O system was increased and fixed to 20 mol%. Pure cubic phases were obtained for the compositions  $(\text{Sc},\text{Y})_{0.2}\text{Zr}_{0.62}\text{Ti}_{0.18}\text{O}_{1.9}$  (Table 1) with further fixed Ti content of 18 mol%. In order to introduce maximum amounts of titanium to achieve higher electronic conductivity, compositions with more titanium (20 mol%) were prepared. A tetragonal second phase was found in the Sc-rich compositions  $\text{Sc}_{0.2}\text{Zr}_{0.6}\text{Ti}_{0.2}\text{O}_{1.9}$  and  $\text{Sc}_{0.15}\text{Y}_{0.05}\text{Zr}_{0.6}\text{Ti}_{0.2}\text{O}_{1.9}$ ; however, a cubic phase was obtained for the Y-rich compositions  $\text{Sc}_{0.1}\text{Y}_{0.1}\text{Zr}_{0.6}\text{Ti}_{0.2}\text{O}_{1.9}$  and  $\text{Sc}_{0.05}\text{Y}_{0.15}\text{Zr}_{0.6}\text{Ti}_{0.2}\text{O}_{1.9}$ . Further increasing the amount of titanium (22 mol%) even for equi molar Sc and Y was demonstrated to be unsuccessful (Table 2). Therefore, mixed doping of scandium and yttrium expands a little the solubility limit of titanium in zirconia to 20 mol% in the Y-rich area. The XRD pattern of cubic  $\text{Sc}_{0.1}\text{Y}_{0.1}\text{Zr}_{0.6}\text{Ti}_{0.2}\text{O}_{1.9}$  obtained at  $1500^\circ\text{C}$  is shown in Fig. 4.

The relationship between lattice parameter and Sc content in cubic  $\text{Sc}_x\text{Y}_{0.2-x}\text{Ti}_{0.18}\text{O}_{1.9}$  is shown in Fig. 5. Area decreased with increasing amount of scandium in the solid solution when yttrium was substituted by the smaller scandium. This change is almost linear with Sc content except for the half-substituted sample  $\text{Sc}_{0.1}\text{Y}_{0.1}\text{Zr}_{0.62}\text{Ti}_{0.18}\text{O}_{1.9}$ , in that there might be some sublattice ordering. Figure 6 shows the temperature dependence of the ionic conductivity of  $(\text{Sc},\text{Y})_{0.2}\text{Zr}_{0.62}\text{Ti}_{0.18}\text{O}_{1.9}$  samples with different Sc/Y ratios. In general, the conductivity is enhanced with increasing amounts of scandium in the system because the size of scandium ions is closer to that of  $\text{Zr}^{4+}$  ions, reducing ion association effects (12, 13). As shown in Fig. 7, the ionic conductivity of  $\text{Sc}_{0.05}\text{Y}_{0.15}\text{Zr}_{0.62}\text{Ti}_{0.18}\text{O}_{1.9}$  is

**TABLE 2**  
**Lattice Parameters and Ionic Conduction Activation Energy of Y-Zr-Ti-O and Sc-Y-Zr-Ti-O Systems**

Composition	$a$ (Å)	Cell volume (Å <sup>3</sup> )	$E_a$ (eV)
$\text{Sc}_{0.2}\text{Zr}_{0.62}\text{Ti}_{0.18}\text{O}_{1.9}$	5.045(1)	128.42(5)	$1.23 \pm 0.02$
$\text{Sc}_{0.15}\text{Y}_{0.05}\text{Zr}_{0.62}\text{Ti}_{0.18}\text{O}_{1.9}$	5.061(2)	129.64(9)	$1.21 \pm 0.02$
$\text{Sc}_{0.1}\text{Y}_{0.1}\text{Zr}_{0.62}\text{Ti}_{0.18}\text{O}_{1.9}$	5.086(1)	131.55(2)	$1.20 \pm 0.02$
$\text{Sc}_{0.05}\text{Y}_{0.15}\text{Zr}_{0.62}\text{Ti}_{0.18}\text{O}_{1.9}$	5.097(1)	132.43(3)	$1.21 \pm 0.01$
$\text{Y}_{0.2}\text{Zr}_{0.62}\text{Ti}_{0.18}\text{O}_{1.9}$	5.111(1)	133.54(2)	$1.18 \pm 0.01$
$\text{Y}_{0.18}\text{Zr}_{0.64}\text{Ti}_{0.18}\text{O}_{1.91}$	5.115(1)	133.81(1)	$1.16 \pm 0.01$
$\text{Y}_{0.16}\text{Zr}_{0.66}\text{Ti}_{0.18}\text{O}_{1.92}$	5.115(1)	133.82(2)	$1.08 \pm 0.03$
$\text{Sc}_{0.1}\text{Y}_{0.1}\text{Zr}_{0.6}\text{Ti}_{0.2}\text{O}_{1.9}$	5.077(5)	130.90(2)	$1.21 \pm 0.01$

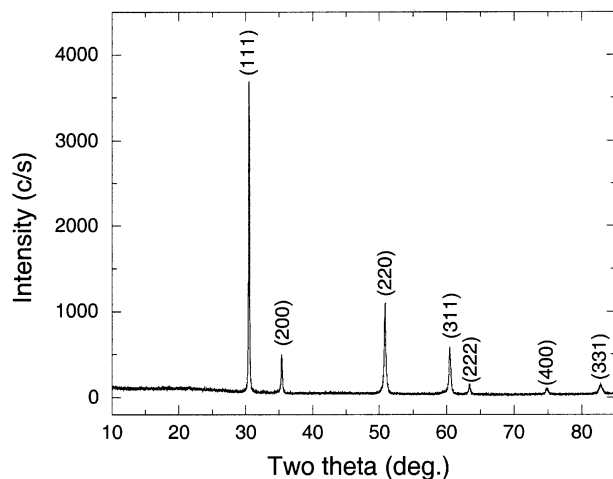


**FIG. 4.** XRD pattern of  $\text{Sc}_{0.1}\text{Y}_{0.1}\text{Zr}_{0.6}\text{Ti}_{0.2}\text{O}_{1.9}$  obtained at  $1500^\circ\text{C}$ .

slightly lower than that of Sc-free  $\text{Y}_{0.2}\text{Zr}_{0.62}\text{Ti}_{0.18}\text{O}_{1.9}$ . Short-range ordering may account for this drop in low ionic conductivity. The conduction activation energy of  $\text{Sc}_{0.05}\text{Y}_{0.15}\text{Zr}_{0.62}\text{Ti}_{0.18}\text{O}_{1.9}$  is also the highest in these samples (Fig. 8), supporting the suggestion that there is increased defect ordering in this composition. With increasing amounts of scandium, the ionic size effect becomes dominant, resulting in enhancement of conductivity. The yttrium-free sample  $\text{Sc}_{0.2}\text{Zr}_{0.62}\text{Ti}_{0.18}\text{O}_{1.9}$  exhibits the highest ionic conductivity.

The electronic conductivities of samples  $(\text{Sc},\text{Y})_{0.2}\text{Zr}_{0.62}\text{Ti}_{0.18}\text{O}_{1.9}$  are shown in Fig. 9. The electronic conductivity increases with temperature. The Sc-containing samples exhibit higher electronic conductivity than  $\text{Y}_{0.2}\text{Zr}_{0.62}\text{Ti}_{0.18}\text{O}_{1.9}$ , which might be due to the shorter hopping distance or smaller lattice parameters. According to this assumption,  $\text{Sc}_{0.2}\text{Zr}_{0.62}\text{Ti}_{0.18}\text{O}_{1.9}$  should exhibit the highest electronic conductivity because its lattice para-

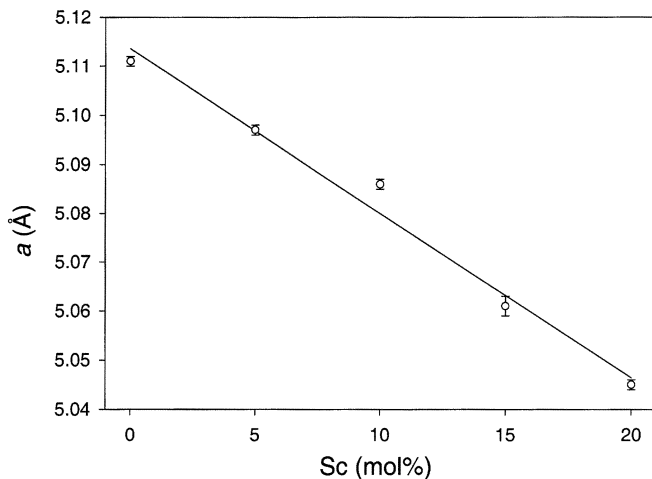


**FIG. 5.** Lattice parameters  $a$  as a function of mol% Sc in  $\text{Sc}_x\text{Y}_{0.2-x}\text{Zr}_{0.62}\text{Ti}_{0.18}\text{O}_{1.9}$ .

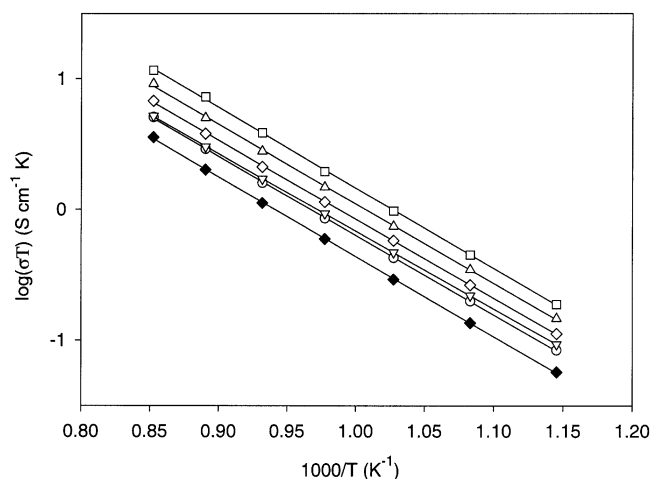


**FIG. 6.** Ionic conductivity of Sc–Y–Zr–Ti–O cubic solid solutions at different temperatures.  $\square$ ,  $\text{Sc}_{0.2}\text{Zr}_{0.62}\text{Ti}_{0.18}\text{O}_{1.9}$ ;  $\triangle$ ,  $\text{Sc}_{0.15}\text{Y}_{0.05}\text{Zr}_{0.62}\text{Ti}_{0.18}\text{O}_{1.9}$ ;  $\diamond$ ,  $\text{Sc}_{0.1}\text{Y}_{0.1}\text{Zr}_{0.62}\text{Ti}_{0.18}\text{O}_{1.9}$ ;  $\circ$ ,  $\text{Sc}_{0.05}\text{Y}_{0.15}\text{Zr}_{0.62}\text{Ti}_{0.18}\text{O}_{1.9}$ ;  $\nabla$ ,  $\text{Y}_{0.2}\text{Zr}_{0.62}\text{Ti}_{0.18}\text{O}_{1.9}$ ;  $\blacklozenge$ ,  $\text{Sc}_{0.1}\text{Y}_{0.1}\text{Zr}_{0.6}\text{Ti}_{0.2}\text{O}_{1.9}$ .

meters are the smallest among the  $(\text{Sc},\text{Y})_{0.2}\text{Zr}_{0.62}\text{Ti}_{0.18}\text{O}_{1.9}$  samples (Fig. 5). The relationship between electronic conductivity and composition of  $(\text{Sc},\text{Y})_{0.2}\text{Zr}_{0.62}\text{Ti}_{0.18}\text{O}_{1.9}$  samples is shown in Fig. 10. Mixed Sc/Y doping samples exhibit higher electronic conductivity than solely Sc- or Y-doped samples when  $x=0$  or  $0.2$ . The deviation seems to be at the Sc-rich and this may well relate to the strong tendency of Sc-rich zirconias to order. Perhaps some short-range ordering causes a deviation from the local cubic structure that reduces conductivity. The highest electronic conductivity,  $1.36 \times 10^{-1}$  S/cm, was observed for  $\text{Sc}_{0.15}\text{Y}_{0.05}\text{Zr}_{0.62}\text{Ti}_{0.18}\text{O}_{1.9}$  at  $900^\circ\text{C}$  among the  $(\text{Sc},\text{Y})_{0.2}\text{Zr}_{0.62}\text{Ti}_{0.18}\text{O}_{1.9}$  samples.

In order to further improve the electronic conductivity, a sample  $\text{Sc}_{0.1}\text{Y}_{0.1}\text{Zr}_{0.6}\text{Ti}_{0.2}\text{O}_{1.9}$  with mixed Sc/Y and max-

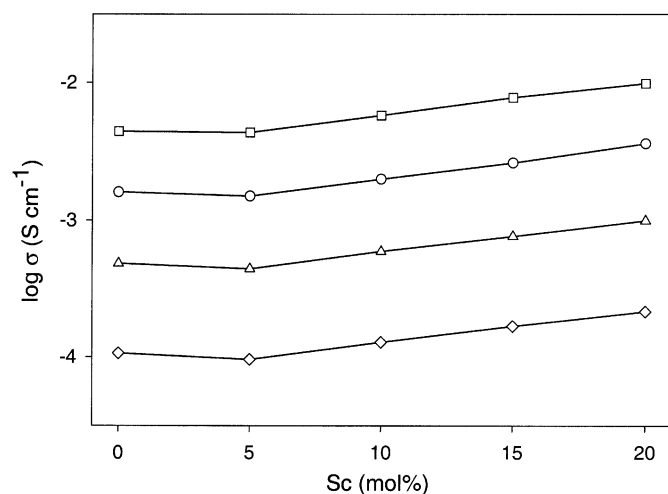


**FIG. 7.** Ionic conductivity as a function of mol% Sc in  $\text{Sc}_x\text{Y}_{0.2-x}\text{Zr}_{0.62}\text{Ti}_{0.18}\text{O}_{1.9}$ .  $\square$ ,  $900^\circ\text{C}$ ;  $\circ$ ,  $800^\circ\text{C}$ ;  $\triangle$ ,  $700^\circ\text{C}$ ;  $\diamond$ ,  $600^\circ\text{C}$ .

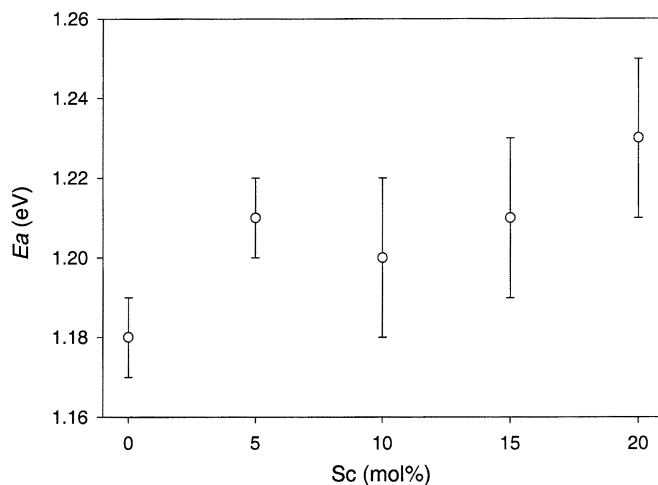


**FIG. 8.** Ionic conduction activation energy as a function of mol% Sc in  $\text{Sc}_x\text{Y}_{0.2-x}\text{Zr}_{0.62}\text{Ti}_{0.18}\text{O}_{1.9}$ .

imum titania (20 mol%) was prepared and its electrical conductivity investigated. As shown in Figs. 6 and 9 respectively, it exhibits lower ionic and higher electronic conductivities than the  $(\text{Sc},\text{Y})_{0.2}\text{Zr}_{0.62}\text{Ti}_{0.18}\text{O}_{1.9}$  samples. The decrease of ionic conductivity when more titanium was introduced could be due to an increased association of oxygen vacancies with the small  $\text{Ti}^{4+}$  ions (20) or due to the increased local strains with  $\text{Ti}^{4+}$  substitution. The electronic conductivity increases a little as there are more titanium atoms in the system to be reduced. It is not easy to find a composition with both high ionic and electronic conductivities in the  $\text{Sc}_2\text{O}_3\text{--Y}_2\text{O}_3\text{--ZrO}_2\text{--TiO}_2$  system. Considering both ionic and electronic conductivities,  $\text{Sc}_{0.15}\text{Y}_{0.05}\text{Zr}_{0.62}\text{Ti}_{0.18}\text{O}_{1.9}$  seems to be a promising SOFC

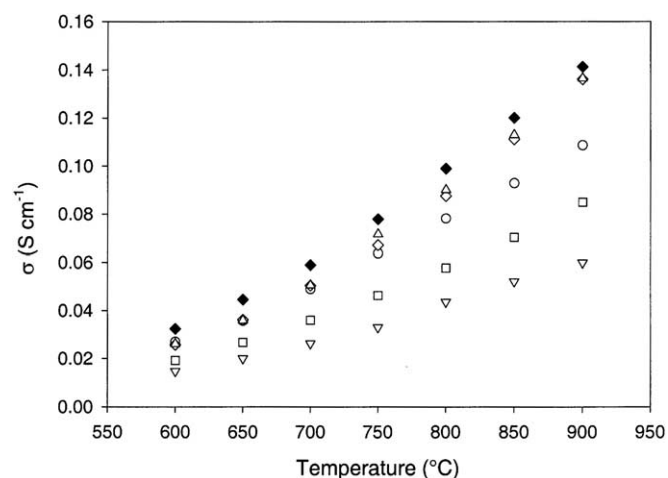


**FIG. 9.** Electronic conductivity of Sc–Y–Zr–Ti–O cubic solid solutions at different temperatures.  $\square$ ,  $\text{Sc}_{0.2}\text{Zr}_{0.62}\text{Ti}_{0.18}\text{O}_{1.9}$ ;  $\triangle$ ,  $\text{Sc}_{0.15}\text{Y}_{0.05}\text{Zr}_{0.62}\text{Ti}_{0.18}\text{O}_{1.9}$ ;  $\diamond$ ,  $\text{Sc}_{0.1}\text{Y}_{0.1}\text{Zr}_{0.62}\text{Ti}_{0.18}\text{O}_{1.9}$ ;  $\circ$ ,  $\text{Sc}_{0.05}\text{Y}_{0.15}\text{Zr}_{0.62}\text{Ti}_{0.18}\text{O}_{1.9}$ ;  $\nabla$ ,  $\text{Y}_{0.2}\text{Zr}_{0.62}\text{Ti}_{0.18}\text{O}_{1.9}$ ;  $\blacklozenge$ ,  $\text{Sc}_{0.1}\text{Y}_{0.1}\text{Zr}_{0.6}\text{Ti}_{0.2}\text{O}_{1.9}$ .

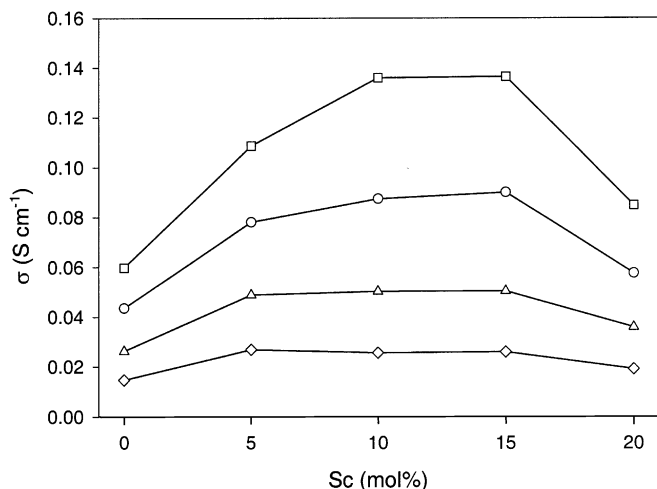


FIG. 10. Electronic conductivity as a function of mol% Sc in  $\text{Sc}_x\text{Y}_{0.2-x}\text{Zr}_{0.62}\text{Ti}_{0.18}\text{O}_{1.9}$ . □, 900°C; ○, 800°C; △, 700°C; ◇, 600°C.

anode material, offering close to the highest electronic and ionic conductivities among the tested samples.

The conductivity change with different  $p\text{O}_2$  was measured by a traditional four-terminal dc method as shown in Fig. 11. It is found that the ionic conduction is dominant until about  $10^{-10}$  atm. The total conductivity increases significantly below  $10^{-10}$  atm. The slope of electronic conductivity change between  $10^{-15}$ – $10^{-18}$  atm is quite close to  $\frac{-1}{4}$  as expected in Section 2. The relative density of this sample is 66%. This makes the measured total and electronic conductivities lower than those measured by The ac method in which a sample with relative density 86% was used.

## 5. CONCLUSIONS

Pure cubic fluorite solid solution phases in the  $\text{Y}_2\text{O}_3$ – $\text{ZrO}_2$ – $\text{TiO}_2$  and  $\text{Y}_2\text{O}_3$ – $\text{Sc}_2\text{O}_3$ – $\text{ZrO}_2$ – $\text{TiO}_2$  systems were

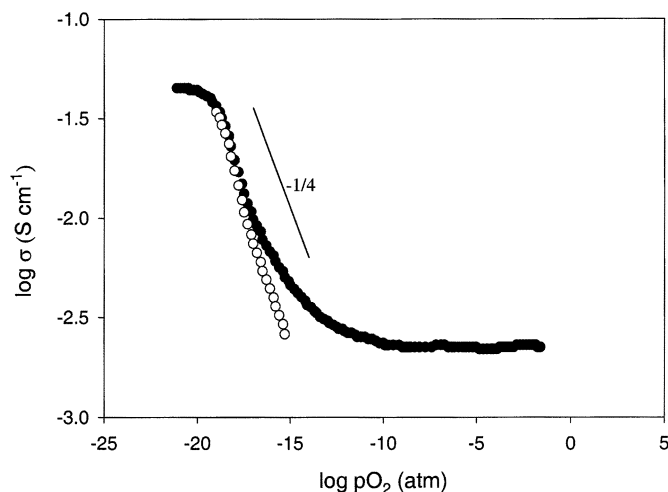


FIG. 11. Dependence of d.c. conductivity of  $\text{Sc}_{0.15}\text{Y}_{0.05}\text{Zr}_{0.62}\text{Ti}_{0.18}\text{O}_{1.9}$  as a function of  $p\text{O}_2$  at 900°C.

prepared by solid state reaction. It was found that  $\text{TiO}_2$  may dissolve to about 18 mol% in ternary systems  $\text{Y}_2\text{O}_3$ – $\text{ZrO}_2$ – $\text{TiO}_2$  and  $\text{Sc}_2\text{O}_3$ – $\text{ZrO}_2$ – $\text{TiO}_2$ , and 20 mol% in the quaternary system  $\text{Sc}_2\text{O}_3$ – $\text{Y}_2\text{O}_3$ – $\text{ZrO}_2$ – $\text{TiO}_2$ . The ionic conductivity is related to the oxygen vacancy concentration and the size of dopant ions, and electronic conductivity to the lattice parameter, the sublattice ordering, and the degree of Ti substitution. Small lattice parameters are beneficial to electron hopping, resulting in higher electronic conductivity. Introduction of scandium into the  $\text{Y}_2\text{O}_3$ – $\text{sZrO}_2$ – $\text{TiO}_2$  system has significantly improved both ionic and electronic conductivities. The highest ionic conductivity ( $1.0 \times 10^{-2}$  S/cm at 900°C) and electronic conductivity (0.14 S/cm at 900°C) were observed for  $\text{Sc}_{0.2}\text{Zr}_{0.62}\text{Ti}_{0.18}\text{O}_{1.9}$  and  $\text{Sc}_{0.1}\text{Y}_{0.1}\text{Zr}_{0.6}\text{Ti}_{0.2}\text{O}_{1.9}$ , respectively. Considering the required levels of both ionic and electronic conductivities for ideal SOFC anode materials,  $\text{Sc}_{0.15}\text{Y}_{0.05}\text{Zr}_{0.62}\text{Ti}_{0.18}\text{O}_{1.9}$  seems to be a promising candidate.

## ACKNOWLEDGMENTS

The authors thank EPSRC and MOD for funding.

## REFERENCES

1. N. Q. Minh, *J. Am. Ceram. Soc.* **76**, 563–588 (1993).
2. N. S. Jacobson and W. L. Worrell, *Proc. High Temp. Mater.* **2**, 217 (1983).
3. B. C. H. Steele, I. Kelly, H. Middleton, and R. Rudkin, *Solid State Ionics* **28–30**, 1547–1552 (1988).
4. A. Kaiser, A. J. Feighery, P. Holtappels, J. L. Bradley, and J. T. S. Irvine, *Solid State Ionics*, submitted.
5. J. T. S. Irvine, D. P. Fagg, J. Labrincha, and F. M. B. Marques, *Catal. Today* **38**, 467–472 (1997).
6. S. W. Tao, Q. Y. Wu, D. K. Peng, and G. Y. Meng, *J. Appl. Electrochem.* **30**, 153–157 (2000).
7. S. S. Liou and W. L. Worrell, *Appl. Phys. A* **49**, 25–31 (1989).
8. H. Naito and H. Arashi, *Solid State Ionics* **53–56**, 436–441 (1992).
9. K. E. Swider and W. L. Worrell, *J. Electrochem. Soc.* **143**, 3706–3711 (1996).
10. A. Kaiser, A. J. Feighery, D. P. Fagg, and J. T. S. Irvine, *Ionics* **4**, 215–219 (1998).
11. A. J. Feighery, J. T. S. Irvine, D. P. Fagg, and A. Kaiser, *J. Solid State Chem.* **143**, 273–276 (1999).
12. S. P. S. Badwal and J. Drennan, *Solid State Ionics* **53–56**, 769–776 (1992).
13. O. Yamamoto, Y. Arati, Y. Takeda, N. Imanishi, Y. Mizutani, M. Kawai, and Y. Nakamura, *Solid State Ionics* **79**, 137–142 (1995).
14. H. Yamamura, N. Utsunomiya, T. Mori, and T. Atake, *Solid State Ionics* **107**, 185–189 (1998).
15. G. Brouwer, *Philips Res. Rep.* **9**, 366 (1954).
16. M. T. Colomer, L. S. M. Tragueia, J. R. Jurado, and F. M. B. Marques, *Mater. Res. Bull.* **30**, 515–522 (1995).
17. S. W. Tao and J. T. S. Irvine, *Mater. Res. Bull.* **36**, 1245–1258 (2001).
18. J. T. S. Irvine, D. C. Sinclair, and A. R. West, *Adv. Mater.* **2**, 132–138 (1990).
19. J. T. S. Irvine, A. J. Feighery, D. P. Fagg, and S. Garcia-Martin, *Solid State Ionics* **136–137**, 879–885 (2000).
20. P. Li, I. W. Chen, and J. E. Penner-Hahn, *J. Am. Ceram. Soc.* **77**, 118–128 (1994).